

High performance RE-Fe-B sintered magnets with high-content misch metal by double main phase process

Yan-Li Liu(刘艳丽), Qiang Ma(马强), Xin Wang(王鑫), Jian-Jun Zhou(周建军), Tong-Yun Zhao(赵同云), Feng-Xia Hu(胡凤霞), Ji-Rong Sun(孙继荣), Bao-Gen Shen(沈保根)

Citation: Chin. Phys. B . 2020, 29(10): 107504 . **doi:** 10.1088/1674-1056/abb3f7
Journal homepage: http://cpb.iphy.ac.cn; http://iopscience.iop.org/cpb

What follows is a list of articles you may be interested in

Degenerate antiferromagnetic states in spinel oxide LiV_2O_4

Ben-Chao Gong(龚本超), Huan-Cheng Yang(杨焕成), Kui Jin(金魁), Kai Liu(刘凯), Zhong-Yi Lu(卢仲毅)
Chin. Phys. B . 2020, 29(7): 077508 . **doi:** 10.1088/1674-1056/ab9617

Gd impurity effect on the magnetic and electronic properties of hexagonal Sr ferrites: A case study by DFT

Masomeh Taghipour, Mohammad Yousefi, Reza Fazaeli, Masoud Darvishganji
Chin. Phys. B . 2020, 29(7): 077505 . **doi:** 10.1088/1674-1056/ab8d9f

Three- and two-dimensional calculations for the interface anisotropy dependence of magnetic properties of exchange-spring $Nd_2Fe_{14}B$/α-Fe multilayers with out-of-plane easy axes

Qian Zhao(赵倩), Xin-Xin He(何鑫鑫), Francois-Jacques Morvan(李文瀚), Guo-Ping Zhao(赵国平), Zhu-Bai Li(李柱柏)
Chin. Phys. B . 2020, 29(3): 037501 . **doi:** 10.1088/1674-1056/ab69e9

Magnetic properties of the double perovskite compound Sr_2YRuO_6

N. EL Mekkaoui, S. Idrissi, S. Mtougui, I. EL Housni, R. Khalladi, S. Ziti, H. Labrim, L. Bahmad
Chin. Phys. B . 2019, 28(9): 097503 . **doi:** 10.1088/1674-1056/ab3441

Influence of misch metal content on microstructure and magnetic properties of R-Fe-B magnets sintered by dual alloy method

Rong-Xiang Shang(商荣翔), Jie-Fu Xiong(熊杰夫), Dan Liu(刘丹), Shu-Lan Zuo(左淑兰), Xin Zhao(赵鑫), Rui Li(李锐), Wen-Liang Zuo(左文亮), Tong-Yun Zhao(赵同云), Ren-Jie Chen(陈仁杰), Ji-Rong Sun(孙继荣), Bao-Gen Shen(沈保根)
Chin. Phys. B . 2017, 26(5): 057502 . **doi:** 10.1088/1674-1056/26/5/057502

High performance RE–Fe–B sintered magnets with high-content misch metal by double main phase process*

Yan-Li Liu(刘艳丽)[1,2,3], Qiang Ma(马强)[1,2], Xin Wang(王鑫)[2], Jian-Jun Zhou(周建军)[2], Tong-Yun Zhao(赵同云)[1,3], Feng-Xia Hu(胡凤霞)[1,3], Ji-Rong Sun(孙继荣)[1,3], and Bao-Gen Shen(沈保根)[1,3,†]

[1] *State Key Laboratory of Magnetism, Institute of Physics, Chinese Academy of Sciences, Beijing* 100190, *China*
[2] *School of Science, Inner Mongolia University of Science and Technology, Baotou* 014010, *China*
[3] *University of Chinese Academy of Sciences, Beijing* 100049, *China*

(Received 21 August 2020; revised manuscript received 26 August 2020; accepted manuscript online 1 September 2020)

Double main phase process is applied to fabricate $[(Pr, Nd)_{1-x}MM_x]_{13.8}Fe_{bal}M_{1.5}B_{5.9}$ ($x = 0.5$ and 0.7; M = Cu, Al, Co, and Nb) sintered magnets with high misch metal (MM) content. In comparison to the magnets by single main phase process, the enhanced magnetic properties have been achieved. For magnets of $x = 0.7$, H_{cj} increases to 371.9 kA/m by 60.5%, and $(BH)_{max}$ is significantly enhanced to 253.3 kJ/m^3 by 56.9%, compared with those of the single main phase magnets of the same nominal composition. In combination with minor loops and magnetic recoil curves, the property improvement of magnets with double main phase method is well explained. As a result, it is demonstrated that double main phase technology is an effective approach to improve the permanent magnetic properties of MM based sintered magnets.

Keywords: misch metal, double main phase process, magnetic properties, coercivity

PACS: 75.47.Np, 75.50.Ww, 75.60.Jk **DOI:** 10.1088/1674-1056/abb3f7

1. Introduction

Due to the outstanding magnetic properties, Nd–Fe–B based permanent magnets have been widely applied in various fields ranging from sensors, hybrid vehicles, wind generators to electronic devices.[1,2] The continuously growing demand of Nd–Fe–B magnets has led to the overspending of the closely-relied Pr, Nd, Dy, and Tb metals, whereas, high abundant La and Ce are overstocked. In order to balance the use of rare earth resources, La or Ce substitution for Nd to prepare RE–Fe–B (RE, rare earth) magnets have attracted worldwide attention again.[3–6] Moreover, the extraction and purifying processes of these elements are very complex and harmful to the environmental security. Therefore, in terms of the environment protection and balanced utilization of rare earth resources, misch metal (MM) with natural ratio[7] (26–29 wt.% La, 49–53 wt.% Ce, 4–6 wt.% Pr, and 15–17 wt.% Nd) from Bayan Obo mine should be directly used to fabricate RE–Fe–B magnets in China.

As shown in the previous studies on Nd–La–Fe–B magnets,[8–11] besides the inferior intrinsic magnetic properties of $La_2Fe_{14}B$ to $Nd_2Fe_{14}B$, there exist troubles in the formation of 2:14:1 tetragonal phase and phase stability at high temperature as well. Hitherto the application of La in RE–Fe–B magnetic material is seriously restrained. Different from La, although Ce is easy to form $Ce_2Fe_{14}B$ phase, yet $CeFe_2$ phase is prone to emerge when the Ce substitution for Nd exceeds 30 at.%.[12,13] On the contrast, for the magnets with La–Ce or MM doping in RE–Fe–B system, $CeFe_2$ phase can be suppressed effectively and more amount of La enters into 2:14:1 phase than that with individual La or Ce substitution.[14] Hence, substitution of MM, composed of nearly 80% La and Ce, for Nd to fabricate RE–Fe–B magnets is believed to be beneficial to improve the overall magnetic performance.

In addition, due to the relatively lower intrinsic magnetic properties of $La_2Fe_{14}B$ (saturation magnetization $\mu_0 M_s$ = 1.38 T, magnetocrystalline field H_A = 2069 kA/m, and Curie temperature T_c = 530 K) and $Ce_2Fe_{14}B$ ($\mu_0 M_s$ = 1.17 T, H_A = 1592 kA/m, and T_c = 424 K) compared to $Nd_2Fe_{14}B$ ($\mu_0 M_s$ = 1.60 T, H_A = 5809 kA/m, and T_c = 585 K),[15,16] the magnetic properties of La, Ce, or MM doping single main phase (SMP) RE–Fe–B magnets deteriorate rapidly with increasing La, Ce, or MM content.[12,17,18] Recently, a novel process known as double main phase (DMP) process has been proposed[3,19–23] to fabricate RE–Fe–B sintered magnets by blending two kinds of powders of different compositions, such as Pr–Nd–Fe–B and La, Ce, or MM based RE–Fe–B, respectively. As a result, the remanence B_r = 1.240 T, the intrinsic coercivity H_{cj} = 716.2 kA/m, and the maximum magnetic energy product $(BH)_{max}$ = 292.0 kJ/m^3 can be obtained at a high Ce substitution level of 45 wt.%.[24] By DMP method, when MM/RE = 30.3 at.%, the sintered RE–Fe–B magnets

*Project supported by the National Natural Foundation of China (Grant Nos. 51590880, 11564030, and 51571126), the National Key Research Program of China (Grant No. 2016YFB0700903), Fujian Institute of Innovation, Chinese Academy of Sciences (Grant No. FJCXY18040302), the Key Program of the Chinese Academy of Sciences (Grant No. KJZD-EW-M05-1), the Inner Mongolia Science and Technology Major Project of 2016, China, and the Natural Science Foundation of Inner Mongolia, China (Grant Nos. 2018LH05006 and 2018LH05011).

†Corresponding author. E-mail: shenbg@iphy.ac.cn

© 2020 Chinese Physical Society and IOP Publishing Ltd

have $H_{cj} = 566$ kA/m and $(BH)_{max} = 326$ kJ/m^3.[22] However, in the MM-based sintered magnets prepared by DMP process, there is no significant enhancement of coercivity as observed in Ce-based sintered magnets fabricated by the same process. And the RE–Fe–B magnetic material with La, Ce, or MM content higher than 50 at.% is rarely investigated so far, the amount of La, Ce, or MM substitution for Nd in RE–Fe–B magnets is usually below 50 at.% in the previous research. Magnetic properties of the sintered RE–Fe–B magnets with a large amount of MM by DMP process need to be further improved to meet the application requirements.

In this work, MM is directly employed to fabricate RE–Fe–B sintered magnets. A Pr–Nd–Fe–B component and an MM–Fe–B component are designed to prepare the RE–Fe–B magnets with DMP process, in which the ratios of MM to RE are 50 at.% and 70 at.%, respectively. The same nominal composition magnets are also manufactured with SMP process for comparison.

2. Experiment

The alloys with the nominal composition of [(Pr, Nd)$_{1-x}$MM$_x$]$_{13.8}$Fe$_{bal}$$M_{1.5}B_{5.9}$ ($x = 0$, 0.5, 0.7, and 1.0), where M refers to Cu, Al, Co, and Nb elements, were prepared by the induction melting and strip casting under high purity argon atmosphere. The raw materials are iron of a purity > 99.5 wt.%, Fe–B alloy with 79.56 wt.% Fe and 19.78 wt.% B, and Pr–Nd alloy of 24.46 wt.% Pr and 75.4 wt.% Nd, as well as M metals and MM of a purity $> 99.5\%$. MM is one kind of the misch metals from Bayan Obo ore with a composition of 28.63 wt.% La, 50.13 wt.% Ce, 4.81 wt.% Pr, 16.28 wt.% Nd, and < 0.05 wt.% the others. Subsequently, the alloy strips were pulverized to powders of average particle size of 3.0–3.5 μm by hydrogen decrepitating and jet-milling process successively. For DMP process, both (Pr, Nd)$_{13.8}$Fe$_{bal}$$M_{1.5}B_{5.9}$ and MM$_{13.8}$Fe$_{bal}$$M_{1.5}B_{5.9}$ powders were blended together according to the preset nominal compositions of [(Pr, Nd)$_{0.5}$MM$_{0.5}$]$_{13.8}$Fe$_{bal}$$M_{1.5}B_{5.9}$ and [(Pr, Nd)$_{0.3}$MM$_{0.7}$]$_{13.8}$Fe$_{bal}$$M_{1.5}B_{5.9}$, respectively. Then, the powders for DMP and SMP processes, respectively, were aligned and compacted under a magnetic field of 2 T and a pressure of ~ 10 MPa, and followed by an isostatic pressing at 200 MPa, and then by sintering at 1020–1060 °C for 2 h. Two-stage annealing of the as-sintered magnets were performed for 2 h at 900 °C and 450–500 °C, respectively. Both sintering and annealing processes were operated in vacuum of $\sim 1 \times 10^{-3}$ Pa.

The permanent magnetic properties of the sintered magnets were tested by the NIM-2000 precision measuring system for hard magnets. The temperature dependence of magnetization, the minor loops, and the recoil curves were measured by a Quantum Design VersaLab at the temperature range of 300–800 K and by a SQUID_VSM at the range of 200–380 K respectively. The microstructure and elements distribution were observed by a SUPRA55 scanning electron microscope (SEM) equipped with energy dispersive x-ray detector (EDX). Elemental concentration mapping was characterized by an EPMA-1720 electron probe micro-analyzer with wavelength dispersive x-ray spectrometer (WDS).

3. Results and discussion

Figure 1(a) presents the room-temperature demagnetization curves for [(Pr, Nd)$_{1-x}$MM$_x$]$_{13.8}$Fe$_{bal}$$M_{1.5}B_{5.9}$ ($x = 0.0$, 0.5, 0.7, and 1.0) sintered magnets prepared by SMP and DMP methods, respectively. The sharp decrease of $(BH)_{max}$ from 382.5 kJ/m^3 to 95.70 kJ/m^3 and the remarkable diminishment of H_{cj} from 1219 kA/m to 111.8 kA/m are observed with increasing MM substitution from $x = 0.0$ to 1.0. The magnetic performance of $x = 1.0$ magnets is better than those reported in the literatures,[20,22,25–27] as illustrated in Fig. 2. Meanwhile, it can be seen that significant enhancements of coercivity, remanence, and maximum magnetic energy product are obtained for magnets with DMP process compared with the SMP ones. For $x = 0.5$, compared with magnets with SMP process of $B_r = 1.245$ T, $H_{cj} = 358.8$ kA/m, and $(BH)_{max} = 242.2$ kJ/m^3, the magnetic performances of magnets with DMP process are $B_r = 1.278$ T, $H_{cj} = 657.9$ kA/m, and $(BH)_{max} = 289.8$ kJ/m^3. For $x = 0.7$, H_{cj} increases from 232.1 kA/m for magnets with SMP process to 371.9 kA/m for magnets with DMP process, B_r also increases from 1.197 T to 1.241 T, and $(BH)_{max}$ is significantly enhanced from 161.4 kJ/m^3 to 253.3 kJ/m^3. It should be noted, as shown in Fig. 1(a), that the permanent magnetic properties of the magnets of $x = 0.7$ with DMP process are even better than those of the magnets of $x = 0.5$ with SMP process unexpectedly, in consideration of the fact of 20 at.% more MM adopted. Figure 1(b) shows the x-ray diffraction (XRD) patterns of the powders from the sintered magnets with SMP and DMP processes. It is obvious that all the samples exhibit the tetragonal 2:14:1 phase. But there exists $CeFe_2$ phase in magnets with SMP process that is harmful to both B_r and H_{cj}, and then $(BH)_{max}$. In one word, when the amount of MM substitution is larger than 50 at.%, magnets with DMP process have relatively better magnetic properties than those with SMP process.

Figure 2 shows the comparison of $(BH)_{max}$ of [(Pr, Nd)$_{1-x}$MM$_x$]$_{13.8}$Fe$_{bal}$$M_{1.5}B_{5.9}$ ($x = 0.0$, 0.5, 0.7, and 1.0) magnets with those of some MM based sintered magnets reported in the literatures.[20,22,25–29] Generally, a dramatic drop of $(BH)_{max}$ occurs when x exceeds 0.5 for all the sintered magnets except the one fabricated by DMP process in this work. It is worthy to note, as mentioned previously, that the sintered magnets of $x = 1.0$, i.e., MM$_{13.8}$Fe$_{bal}$$M_{1.5}B_{5.9}$ magnets in this

work show the highest $(BH)_{max}$ to date, it is reasonable to conclude that the excellent magnetic performances of the sintered magnets by DMP process in this work probably could be attributed to the superior magnetic properties of the original alloy of $MM_{13.8}Fe_{bal}M_{1.5}B_{5.9}$.

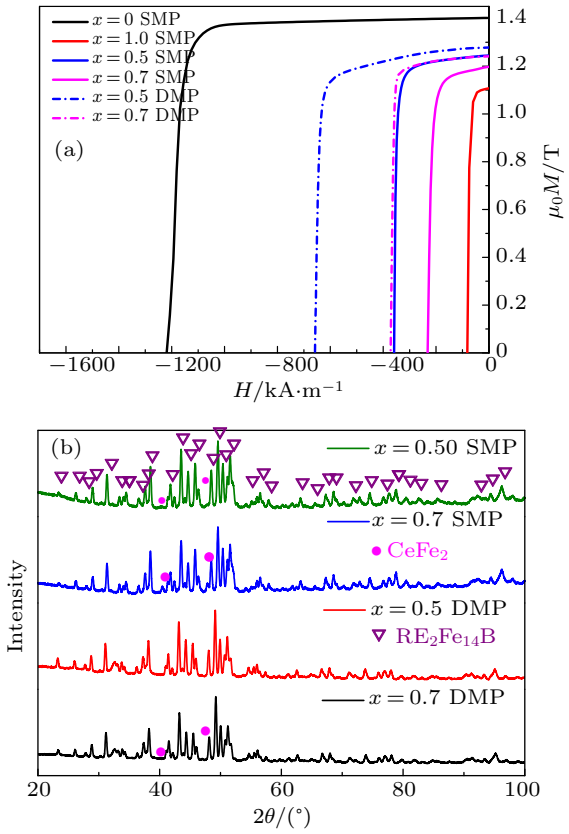


Fig. 1. (a) The room-temperature demagnetization curves of the $[(Pr, Nd)_{1-x}MM_x]_{13.8}Fe_{bal}M_{1.5}B_{5.9}$ ($x = 0.0$, 0.5, 0.7, and 1.0) magnets. (b) XRD patterns of the sintered magnet prepared by SMP or DMP process.

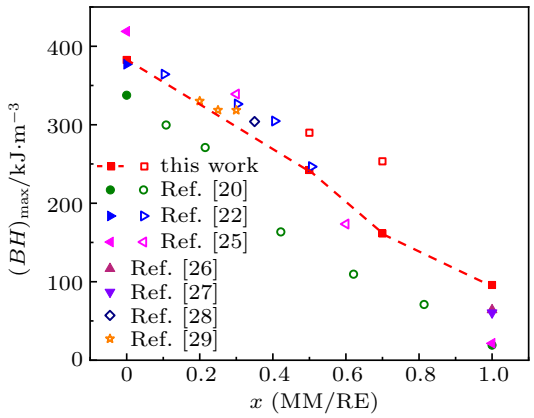


Fig. 2. The comparison of $(BH)_{max}$ for MM based RE–Fe–B sintered magnets. The solid and hollow symbols are corresponding to SMP and DMP processes, respectively.

Due to the similar lattice parameters of the $[(Pr, Nd)_{1-x}MM_x]_{13.8}Fe_{bal}M_{1.5}B_{5.9}$ magnets, it is difficult to identify the main phase components by XRD solely. Hence, the temperature dependence of magnetization for the $[(Pr, Nd)_{1-x}MM_x]_{13.8}Fe_{bal}M_{1.5}B_{5.9}$ ($x = 0.5$ and 0.7) magnets with DMP process was measured, as shown in Fig. 3, with an applied magnetic field of 23.8 kA/m in a temperature range of 300–700 K. The plots of $d\sigma_m/dT$ vs. temperature T, which are employed to determine the Curie temperatures of the magnets, are displayed in red lines in Fig. 3. In magnets by DMP process, three Curie temperatures, labeled as T_{c1}, T_{c2}, and T_{c3}, respectively, are observed for both $x = 0.5$ and 0.7. With the content of MM increasing from 0.5 to 0.7, the Curie temperatures of T_{c1}, T_{c2}, and T_{c3} decrease from 526.2 K, 568.0 K, and 603.0 K to 521.0 K, 558.2 K, and 589.1 K, respectively. The value of T_{c2} is close to T_c of the magnets by SMP process in our previous study,[30] but T_{c1} and T_{c2} are similar to those of $MM_2(Fe, Co)_{14}B$ and $(Pr, Nd)_2(Fe, Co)_{14}B$, respectively. Since the Curie temperature of magnets intensively depends on the composition,[31] the occurrence of three Curie temperatures indicates that there should be three magnetic phases with different La, Ce, Pr, and Nd as well as Fe concentration in the magnets with DMP process. It is probably resulted from the element diffusion among the main grains during the sintering process, and a kind of construction with multiple main phases is synthesized in the magnets during the DMP preparation process, which is completely different from the sintered magnets with SMP process.

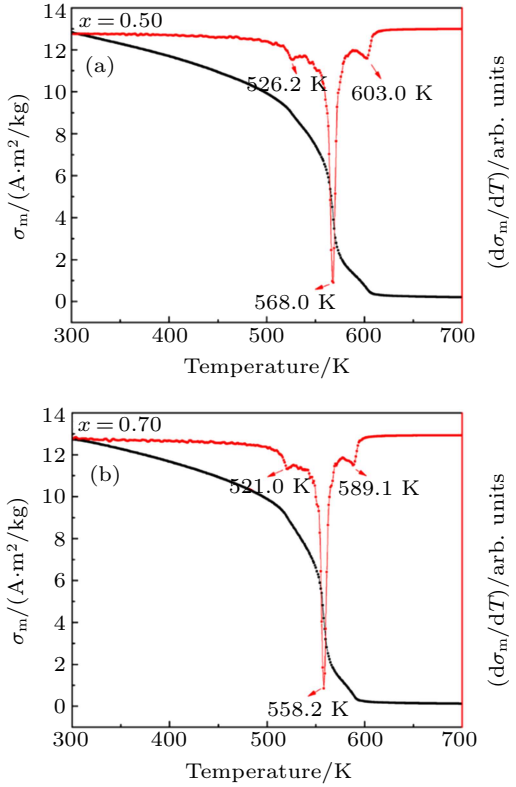


Fig. 3. Temperature dependence of σ_m and $d\sigma_m/dT$ in the range of 300–700 K for $[(Pr, Nd)_{1-x}MM_x]_{13.8}Fe_{bal}M_{1.5}B_{5.9}$ ($x = 0.5$ and 0.7) magnets prepared by DMP process.

Figure 4 illustrates the back-scattered images of $[(Pr, Nd)_{1-x}MM_x]_{13.8}Fe_{bal}M_{1.5}B_{5.9}$ ($x = 0.5$ and 0.7) magnets prepared by SMP and DMP processes, respectively. The dark

gray region in Fig. 4 is $RE_2Fe_{14}B$ matrix phase, and the bright region corresponds to RE-rich intergranular phase. It can be seen that magnets with DMP process (Figs. 4(b) and 4(d)) have more continuous RE-rich phase layers surrounding the main grains compared with the magnets with SMP process (Figs. 4(a) and 4(c)). On the contrast, for the magnets with SMP process, the RE-rich phase is prone to aggregate in grain boundary triple junctions. It is well known that the nucleation of reversed domains is prone to occur at the tripe junctions, thus the lower coercivity is found in magnets with SMP but not DMP process. In addition, as shown in Figs. 4(b) and 4(d), most of the grains show a clear contrast between core and shell for the magnets with DMP process. The shell region is darker than the core region, suggesting elements of smaller average atomic numbers existing in the shell rather than in the core, it implies that Pr and Nd are left in the core region, meanwhile, La and Ce diffuse to the shell region, therefore the grains in the DMP magnets are composed of a magnetically soft shell around a magnetically hard core region. With higher Pr and Nd contents, the core region bears both high magnetocrystalline anisotropy field and the saturation magnetization, compared to the homogeneous magnets with SMP process. All above factors are beneficial to yield better magnetic properties for magnets with DMP process.

In order to further confirm the difference of the element distribution between magnets with SMP and DMP processes, the back-scattered electron image and corresponding mapping profile of La, Ce, Pr, Nd, and Fe elements are detected and illustrated in Figs. 5 and 6. For magnets with SMP process, the concentration distributions of La, Ce, Pr, and Nd within the main phase are uniform as shown in Fig. 5. Comparatively, as shown in Fig. 6, there are obvious rare earth element distribution heterogeneities both within one individual grain and between inter grains for magnets with DMP process. As a result of composition difference between two kinds of original powders of $(Pr, Nd)_{13.8}Fe_{bal}M_{1.5}B_{5.9}$ and $MM_{13.8}Fe_{bal}M_{1.5}B_{5.9}$, both Pr and Nd elements diffuse from $(Pr, Nd)_2(Fe, M)_{14}B$ grains into $MM_2(Fe, M)_{14}B$ grains, meanwhile, both La and Ce migrate oppositely. Core–shell structures, labeled as area A, are also obviously found in Figs. 6(b) and 6(c), La and Ce ions in MM have diffused into the surface layer of $(Pr, Nd)_2(Fe, M)_{14}B$ grains, at the same time, Pr and Nd occupy the positions of La and Ce, as shown in labeled area B.

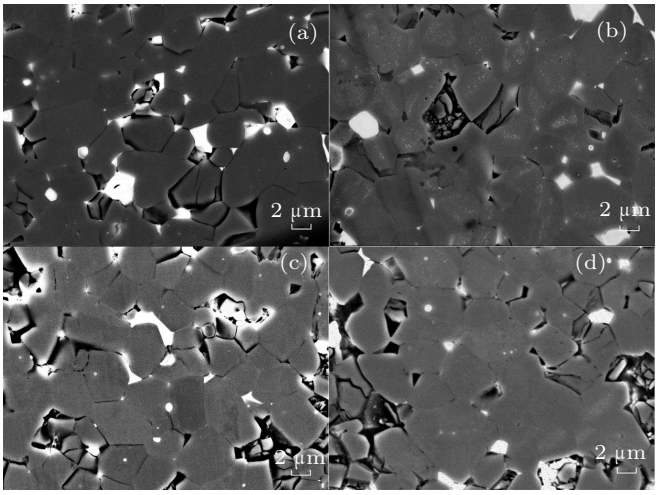


Fig. 4. The back-scattered images of $[(Pr, Nd)_{1-x}MM_x]_{13.8}Fe_{bal}M_{1.5}B_{5.9}$ magnets: (a) $x = 0.5$ with SMP, (b) $x = 0.5$ with DMP, (c) $x = 0.7$ with SMP, and (d) $x = 0.7$ with DMP process.

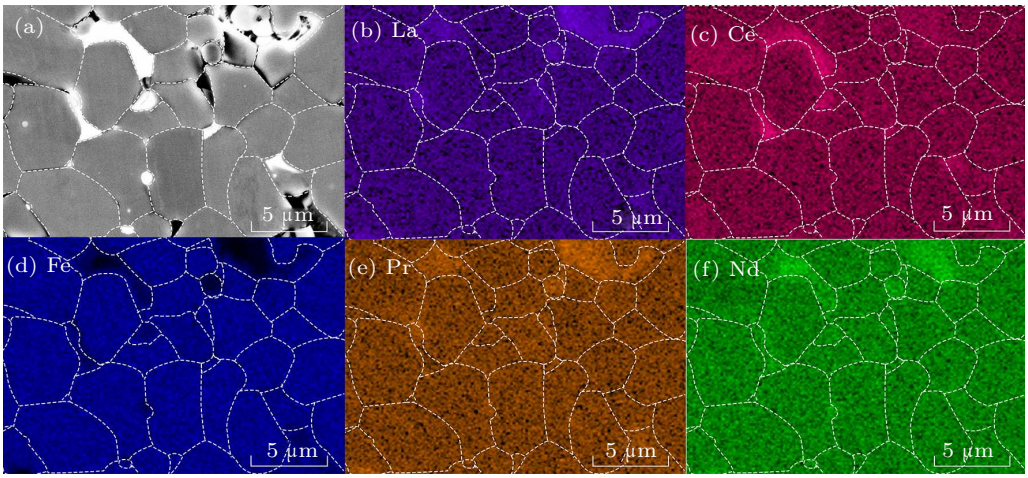


Fig. 5. (a) Back-scattered electron image and (b)–(f) the corresponding EDX mappings of La, Ce, Fe, Pr, and Nd for $[(Pr, Nd)_{0.3}MM_{0.7}]_{13.8}Fe_{bal}M_{1.5}B_{5.9}$ magnets with SMP process.

The plots of the reduced magnetization M/M_{max}, coercivity $H_{cj}/H_{cj,max}$, and remanence $M_r/M_{r,max}$, obtained from the minor hysteresis loops (the insets in Fig. 7), versus the reduced maximum applied field H/H_{cj} are shown in Fig. 7. For magnets with DMP process, M/M_{max} increases rapidly until the applied field H exceeds $0.5H_{cj}$, then follows by a steep rise when H is approaching to H_{cj}. This phenomenon may be resulted from the pinning effect of domain wall during the magnetization process. But the pinning effect is weaker than that found in the nanostructural magnetic materials, because

$H_{cj}/H_{cj,max}$ increases faster than $M_r/M_{r,max}$ when H just exceeds H_{cj}. However, there is no such feature observed for magnets with SMP process. It may be attributed to heterogeneity of rare earth element distribution in magnets with DMP process, which leads to differences of the anisotropy fields in local regions. Due to the exchange couplings of these local regions, the magnetic properties of magnets with DMP process are enhanced considerably.

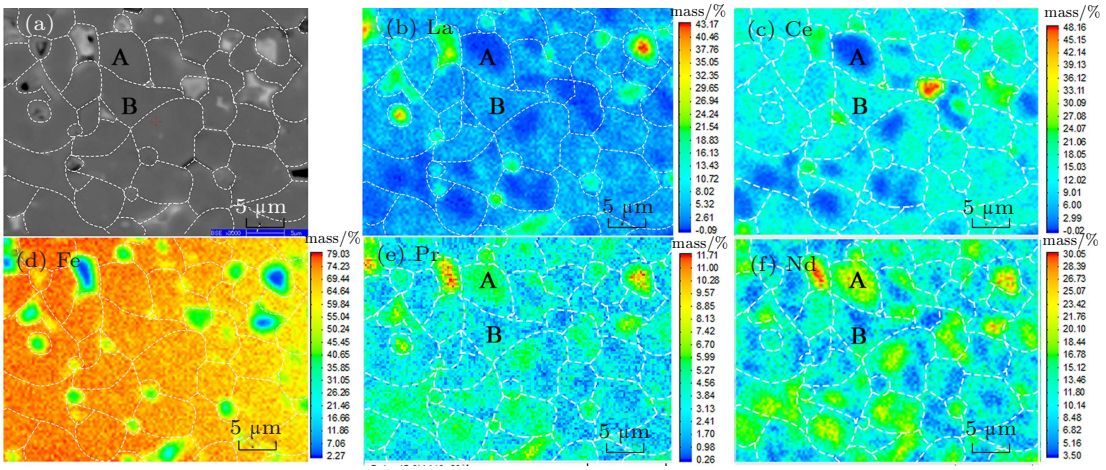


Fig. 6. (a) Back-scattered electron image and (b)–(f) the corresponding EPMA mappings of La, Ce, Fe, Pr, and Nd for $[(Pr, Nd)_{0.3}MM_{0.7}]_{13.8}Fe_{bal}M_{1.5}B_{5.9}$ DMP magnets.

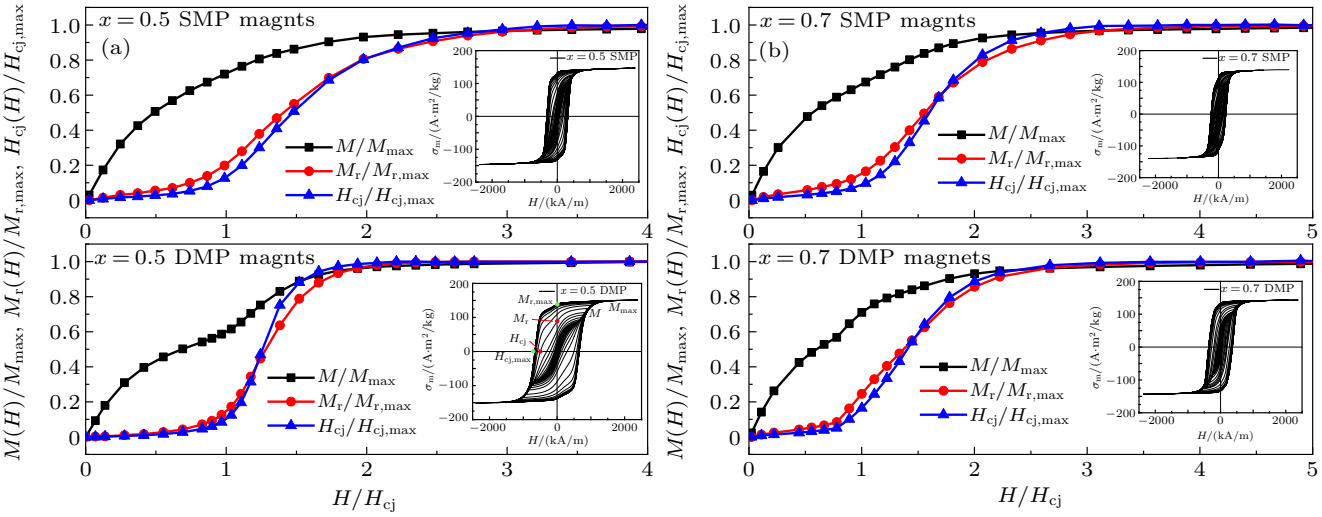


Fig. 7. The dependence of M, M_r, and H_{cj} of minor loops of $[(Pr, Nd)_{1-x}MM_x]_{13.8}Fe_{bal}M_{1.5}B_{5.9}$ magnets on H/H_{cj} for (a) $x = 0.5$ and (b) $x = 0.7$, the insets show the minor loops.

Recoil curves in demagnetization process are tested for both DMP and SMP $[(Pr, Nd)_{1-x}MM_x]_{13.8}Fe_{bal}M_{1.5}B_{5.9}$ ($x =$ 0.5 and 0.7) magnets, as shown in Fig. 8. The recoil curves of the SMP and DMP magnets show the tadpole-like openness which is related to the irreversible magnetization. Compared with magnets with SMP process, the openness is relatively small in magnets with DMP process, which represents the larger magnetic hardness. The reversible specific susceptibility χ_{rev}/σ_s, as illustrated in Fig. 9, is defined as $[\sigma_d(H) - \sigma_m(H)]/(\sigma_s H)$, where $\sigma_d(H)$ and $\sigma_m(H)$ are the values of specific magnetization after and before the removal of the applied reverse magnetic field H, respectively, and σ_s is the specific remanent magnetization. The deduced χ_{rev}/σ_s versus the applied field is shown in Fig. 9(b), which is proposed to reveal the strength of the exchange coupling.[32] Compared with DMP magnets, the higher peak value of χ_{rev}/σ_s of the magnets with SMP process indicates that their magnetic moment is easy to be reversed under a lower applied field. The relative strong exchange coupling among grains with different anisotropy fields in local regions in magnets with DMP process strengthens the magnetic moment alignment after removing magnetizing field, and the uniformity of the magnetic moment reversal is enhanced.[33] Combined with the fact that the grains of the main phase are perfectly aligned in the sintered magnets with DMP process verified by the XRD technique (not presented here), both B_r and H_{cj} of the magnets with DMP process are improved compared with the ones by SMP method.

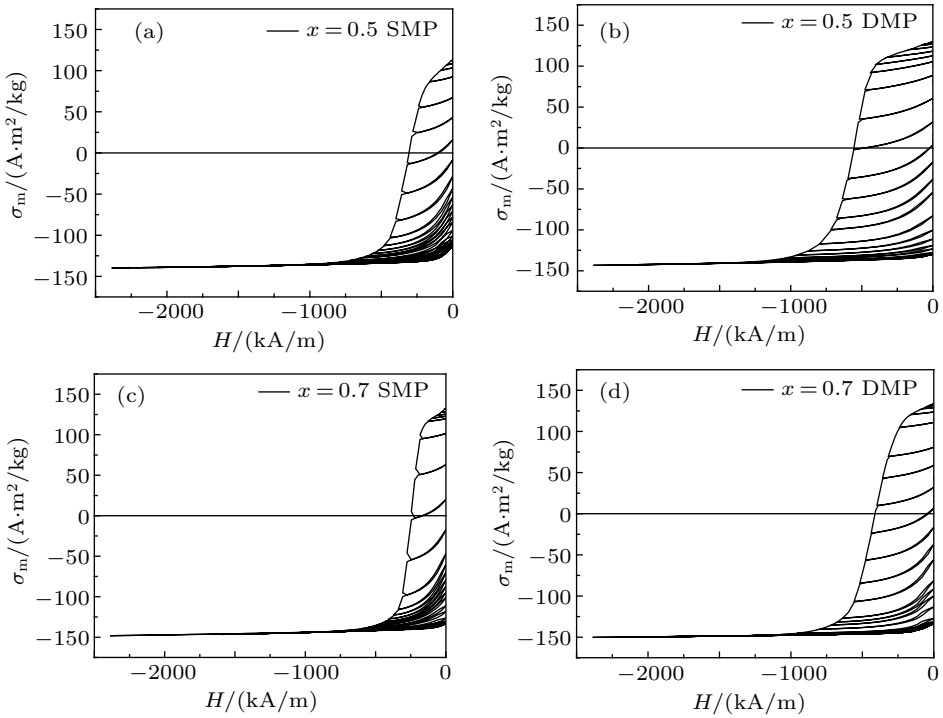


Fig. 8. The recoil loops for $[(Pr, Nd)_{1-x}MM_x]_{13.8}Fe_{bal}M_{1.5}B_{5.9}$ ($x = 0.5$ and 0.7) magnets with SMP and DMP processes, respectively.

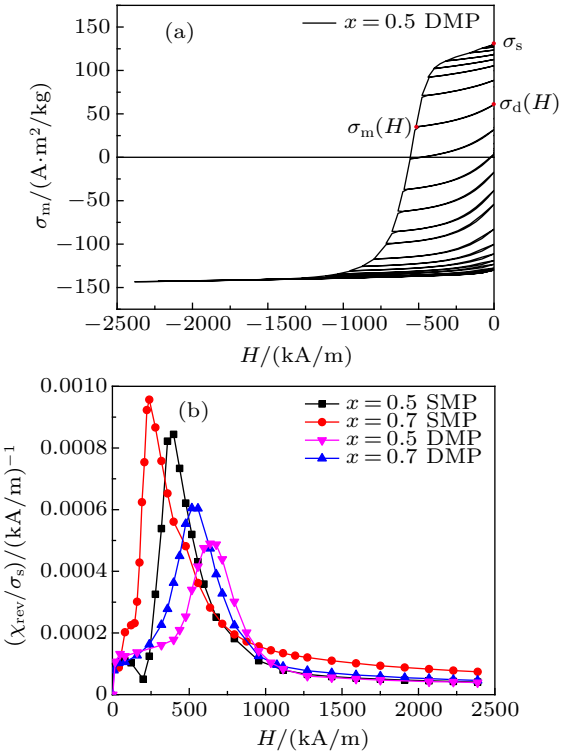


Fig. 9. (a) The recoil loops for $[(Pr, Nd)_{0.5}MM_{0.5}]_{13.8}Fe_{bal}M_{1.5}B_{5.9}$ DMP magnets, (b) the dependence of χ_{rev}/σ_s on the applied magnetic field H deduced from the recoil loops for $[(Pr, Nd)_{1-x}MM_x]_{13.8}Fe_{bal}M_{1.5}B_{5.9}$ ($x = 0.5$ and 0.7) magnets with SMP and DMP processes, respectively.

4. Conclusion and perspectives

In this work, the DMP and SMP processes are employed to fabricate the $[(Pr, Nd)_{1-x}MM_x]_{13.8}Fe_{bal}M_{1.5}B_{5.9}$ ($x = 0.0$, 0.5 0.7, and 1.0) sintered magnets with high MM content. The magnets prepared by DMP method exhibit much better magnetic properties than those by SMP method. When x is equal to 0.7, H_{cj} increases from 232.1 kA/m of magnets with SMP process to 371.9 kA/m of magnets with DMP process, B_r also increases from 1.197 T to 1.241 T, and $(BH)_{max}$ is enhanced significantly from 161.4 kJ/m^3 to 253.3 kJ/m^3. In addition, magnets of high content of MM ($x \geq 0.5$) with DMP process appears to be of multiple main phase construction. The enhancement of magnetic performance of the magnets with DMP process could be contributed to the strong exchange coupling among adjacent grains with different magnetocrystalline fields and the pinning effect.

References

[1] Sagawa M, Fujimura S, Togawa N, Yamamoto H and Matsuura Y 1984 *J. Appl. Phys.* **55** 2083
[2] Hu B P, Niu E, Zhao Y G, Chen G A, Chen Z A, Jin G S, Zhang J, Rao X L and Wang Z X 2013 *AIP Adv.* **3** 042136
[3] Zhu M G, Han R, Li W, Huang S L, Zheng D W, Song L W, and Shi X N 2015 *IEEE Trans. Magn.* **51** 2104604
[4] Li Z B, Shen B G, Zhang M, Hu F X and Sun J R 2015 *J. Alloys Compd.* **628** 325
[5] Jin J Y, Wang Z, Bai G H, Peng B X, Liu Y S and Yan M 2018 *J. Alloy. Compd.* **749** 580
[6] Li Z, Liu W Q, Zha S S, Li Y Q, Wang Y Q, Zhang D T, Yue M and Zhang J X 2015 *J. Rare Earths* **33** 961
[7] Zuo W L, Zuo S L, Li R, Zhao T Y, Hu F X, Sun J R, Zhang X F, Liu J P and Shen B G 2017 *J. Alloy. Compd.* **695** 1786
[8] Stadelmaier H H, Liu N C and Elmasry N A 1985 *Mater. Lett.* **3** 130
[9] Hadjipanayis G C, Tao Y F and Gudimetta K 1985 *Appl. Phys. Lett.* **47** 757
[10] Wei Q, Lu Z, Wang J, Yao Q R, Long Q X, Qin M and Zhou H Y 2020 *J. Phase Equilib. Diffus.* **41** 35
[11] Herbst J F, Meyer M S and Pinkerton F E 2012 *J. Appl. Phys.* **111** 07A718
[12] Yan C J, Guo S, Chen R J, Lee D and Yan A R 2014 *IEEE Trans. Magn.* **50** 2102605

[13] Lu Q M, Niu J, Liu W Q, Yue M and Altounian Z 2017 *IEEE Trans. Magn.* **53** 2100603
[14] Zhang M, Li Z B, Shen B G, Hu F X and Sun J R 2015 *J. Alloys Compd.* **651** 144
[15] Herbst J F 1991 *Rev. Mod. Phys.* **63** 819
[16] Hirosawa S, Matsuura Y, Yamamoto H, Fujimura S, Sagawa M and Yamauchi H 1986 *J. Appl. Phys.* **59** 873
[17] Liao X F, Zhao L Z, Zhang J S, Zhong X C, Jiao D L and Liu Z W 2018 *J. Magn. Magn. Mater.* **464** 31
[18] Zhang X F, Shi Y, Ma Q, Liu Y L, Shi M F, Li Y F, Wang G F and Zhao Z R 2015 *Rare Metal Mat. Eng.* **44** 748
[19] Zhu M G, Li W, Wang J D, Zheng L Y, Li Y F, Zhang K, Feng H B and Liu T 2014 *IEEE Trans. Magn.* **50** 1000104
[20] Niu E, Chen Z A, Chen G A, Zhao Y G, Zhang J, Rao X L, Hu B P and Wang Z X 2014 *J. Appl. Phys.* **115** 113912
[21] Jin J Y, Ma T Y, Zhang Y J, Bai G H and Yan M 2016 *Sci. Rep.* **6** 32200
[22] Shang R X, Xiong J F, Liu D, Zuo S L, Zhao X, Li R, Zuo W L, Zhao T Y, Chen R J, Sun J R and Shen B G 2017 *Chin. Phys. B* **26** 057502
[23] Lai R S, Chen R J, Yin W Z, Tang X, Wang Z X, Jin C X, Lee D and Yan A R 2017 *J. Alloys Compd.* **724** 275
[24] Zhang Y J, Ma T Y, Jin J Y, Li J T, Wu C, Shen B G and Yan M 2017 *Acta Mater.* **128** 22
[25] Yu X Q 2018 *Study on structure, magntic properties and magnetic hardening mechanism of sintered permanent magnets based on misch metal* (Ph. D. dissertation) (Beijing: Beijing University of Technology) (in Chinese), Chapter 5, pp. 76–80
[26] Liu W Q, Zhang Z P, Yue M, Li Z, Wu D, Zhou Z, Chen H, Li Y Q, Pang Z S and Yu X 2019 *Intermetallics* **115** 106626
[27] Shang R X, Xiong J F, Li R, Zuo W L, Zhang J, Zhao T Y, Chen R J, Sun J R and Shen B G 2017 *AIP Adv.* **7** 056215
[28] Chen H, Liu W Q, Yin Y T, Li Z, Wang Z J, Li Y Q, Yue M, Pang Z S, Yu X and Yu C H 2020 *Intermetallics* **124** 106870
[29] Ma Q, Zhu J T, Zhang X F, Zhao Z R, Liu Y L, Wang G F, Li Y F and Li Z B 2018 *Rare Metals* **37** 237
[30] Liu Y L, Zhou J J, Wang X, Ma Q, Liu F, Liu J, Zhao T Y, Hu F X, Sun J R and Shen B G 2020 *J. Magn. Magn. Mater.* **513** 167162
[31] Sepehri-Amin H, Liu L H, Ohkubo T, Yano M, Shoji T, Kato A, Schrefl T and Hono K 2015 *Acta Mater.* **99** 297
[32] Li Z B, Shen B G and Sun, J R 2013 *J. Appl. Phys.* **113** 013902
[33] Fan X D, Guo S, Chen K, Chen R J, Lee D, You C Y and Yan A R 2016 *J. Magn. Magn. Mater.* **419** 394